REDESIGN OF THE END GROUP IN THE 3.9 GHz LCLS-II CAVITY*

A. Lunin†, I. Gonin, T. Khabiboulline, N. Solyak, Fermi National Accelerator Laboratory, Batavia, USA

Abstract

Development and production of Linac Coherent Light Source II (LCLS-II) is underway. The central part of LCLS-II is a continuous wave superconducting RF (CW SCRF) electron linac. The 3.9 GHz third harmonic cavity similar to the XFEL design will be used in the linac for linearizing the longitudinal beam profile [1]. The initial design of the 3.9 GHz cavity developed for the XFEL project has a large, 40 mm, beam pipe aperture for ensuring a low (< 10^6) cavity loaded quality factor. It is resulted in dipole HOMs with frequencies nearby the operating mode, which causes difficulties with HOM coupler notch filter tuning. The CW linac operation requires an extra caution in the design of the HOM coupler in order to prevent its possible overheating. In this paper, we present the modified 3.9 GHz cavity End Group for meeting to the LCLS-II requirements.

INTRODUCTION

A continuous operation regime of the 3.9 GHz LCSL-II accelerating structure at the maximum gradient of 14.9 MV/m sets an extra caution on possible overheating of HOM couplers feedthroughs [2, 3]. The HOM feedthrough coupling antenna is made of a solid Niobium, which does not produce significant amount of RF losses until its temperature is keeping below critical, but it may initiate a thermal runaway process and end up by a cavity quench due to a leak of an operating mode or a resonant excitation of the cavity HOM spectrum [4]. In order to avoid such a scenario, one has to minimize the antenna RF heating by using smaller antenna tip and increasing the size of the f-part snag. The proposed HOM coupler modification in the 3.9 GHz cavity is illustrated in Fig. 1. The height of antenna tip is decreased from 5 mm to 1 mm and the height of the f-part snag is increased to 7.8 mm in order to make a shallow antenna penetration and, thus, to lower a surface magnetic field. The nominal gap between the antenna and the f-part is chosen equal to 0.5 mm.

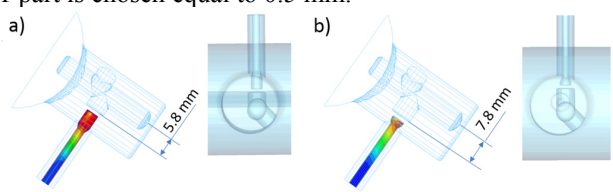

Figure 1: Modifications of the HOM coupler for the 3.9 GHz cavity: a) XFEL design and b) LCLS-II design.

Another drawback of the original XFEL End Group design is an oversized 40 mm aperture of the beam pipe, which has a cut off frequency of the lowest dipole mode very close to an operating mode. Eventually it makes quite difficult tuning the HOM coupler notch filter in a close proximity of dipole HOMs in the cavity End Group [5]. As a remedy, we decided to decrease slightly both apertures of the beam pipe and interconnecting bellows to 38 mm aiming to shift up frequencies of nearby dipole HOMs by at least of 100 MHz Modified design of the 3.9 GHz cavity End Group is illustrated in Fig. 2. The geometry of the cavity end cell remains untouched, while the tapering to a smaller aperture is made within the Nb transition ring.

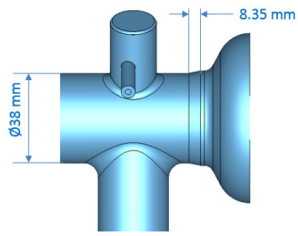

Figure 2: New design of the 3.9 GHz cavity End Group.

OPERATING MODE RF LOSSES

Parameters of operating mode for both designs of 3.9 GHz cavities, XFEL and LCLS-II, are compared in the Table 1. Since only the End Group was modified, there are little changes in the cavity performance

Table 1: Parameters of 3.9 GHz Cavities

Operating Mode Parameters	XFEL	LCLS-II
Frequency, [GHz]	3.9	3.9
Stored Energy, [J]	1	1
R/Q, [Ω]	746	751
Effective Length, [m]	0.346	0.346
Max Electric Field on Axis, [MV/m]	25.4	25.3
Accelerating Gradient, [MV/m]	12.36	12.40
Normalized Surface Electric Field	2.25	2.24
Normalized Surface Magnetic Field, [mT/MV/m]	4.90	4.88

A tail of the operating mode decays to the beam pipe and a remnant surface magnetic field causes ohmic losses in the bellows and connecting flanges. We used ANSYS HFSS software for electromagnetic simulations of the 3.9 GHz cavity [6]. A mechanical model of cavity and bellows connection as well as a distribution of the magnetic field penetrating to the beam pipe are shown in Fig. 3. The result of local G-factors calculations and associated RF losses in the

* Operated by Fermi Research Alliance, LLC under Contract No. DE-AC02-07CH11359 with the United States Department of Energy.
† lunin@fnal.gov

ISBN 978-3-95450-169-4

End Group at the accelerating gradient of 14.9 MV/m are summarized in Table 2. One can see that the length of the cavity End Group is long enough for a substantial attenuation of the magnetic field and the expected operating mode RF loss for a non-plated stainless steel bellows is only an order of tens of milliwatts.

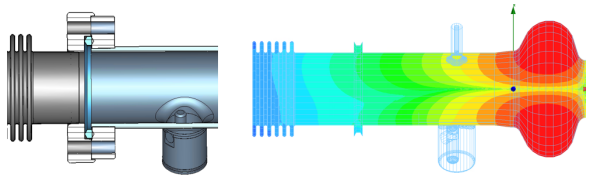

Figure 3: Mechanical 3D model of cavity and bellows connection (left) and operating mode magnetic field (right)

Table 2: Operating Mode RF Losses in the End Group

End Group Component	G-Factor	RF Loss, [mW]	
		Copper (RRR=15)	Steel (316LN)
Bellows Body (Upstream)	$2.1\text{x}10^{11}$	0.9	18
Bellows Body (Downstream)	$1.4\text{x}10^{11}$	1.4	28
Bellows Flange (Upstream)	$9.2\text{x}10^{11}$	0.2	5
Bellows Flange (Downstream)	$5.6\text{x}10^{11}$	0.3	7
HOM antenna	$3.2\text{x}10^{8}$ (XFEL) $1.7\text{x}10^{9}$ (LCLS-II)	-	

In the tuned HOM coupler, the feedthrough antenna with new tip has a higher local G-factor of $1.7\text{x}10^{9}$, comparing to the $3.2\text{x}10^{8}$ G-factor of the original design. It is equivalent to a reduction by a factor of five of associated surface RF losses, which makes new HOM coupler suitable for the CW operation.

DIPOLE HOMS SPECTRUM

A large beam pipe with an aperture of 40 mm gives an advantage for efficient HOMs damping but, at the same time, it bring frequencies of dipole HOMs close to the cavity operating mode. Maps of electric field for nearby dipole HOMs in the cavity End Group and interconnecting bellows are shown in Fig. 4 for the XFEL 3.9 GHz cavity. Properties of first six modes trapped between two cavities are presented in Table 3 based on ANSYS HFSS simulations. External quality factors are calculated for perfectly matched power and HOM couplers. The frequency of the closest dipole mode is only 92 MHz above the operating frequency of 3.9 GHz. Taking into account cavity mechanical tolerances, a further frequency decrease after chemical polishing and low quality factors of dipole modes, it makes a problematic tuning of the HOM coupler notch filter at room temperature.

Table 3: Dipole HOMs of the XFEL 3.9 GHz cavity.

Mode #	Frequency [GHz]	Q_{ext}	$(R/Q)_x$ [Ω/mm^2]	$(R/Q)_y$ [Ω/mm^2]
1	3.992	3.6e4	0.06	0.26
2	4.047	8.0e4	0.02	5e-3
3	4.059	2.5e5	5e-3	0.34
4	4.136	5.9e3	1.0	0.96
5	4.135	4.9e3	7.3	3.0
6	4.150	3.3e5	1.2	1.6

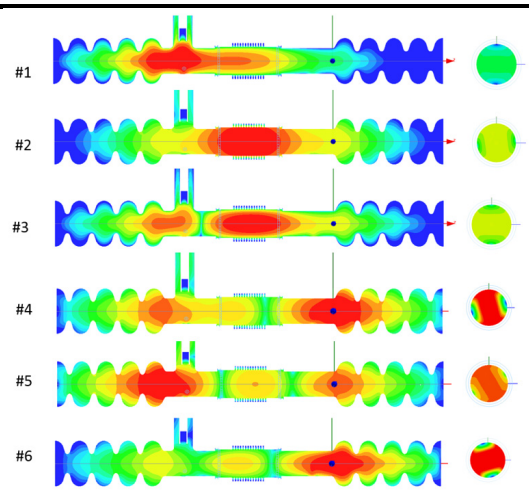

Figure 4: Electric fields (log scale) of dipole HOMs in the XFEL 3.9 GHz cavity End Group.

Table 4: Dipole HOMs of the XFEL 3.9 GHz cavity

Mode #	Frequency [GHz]	Q_{ext}	$(R/Q)_x$ [Ω/mm^2]	$(R/Q)_y$ [Ω/mm^2]
1	3.992	3.6e4	0.06	0.26
2	4.047	8.0e4	0.02	5e-3
3	4.059	2.5e5	5e-3	0.34
4	4.136	5.9e3	1.0	0.96

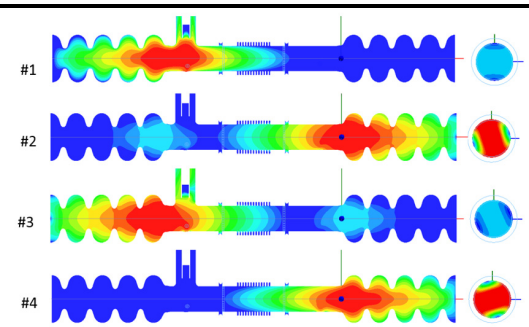

Figure 5: Electric fields (log scale) of dipole HOMs in the LCLS-II 3.9 GHz cavity End Group.

For the LCLS-II linac, it is decided to reduce the aperture of a beam pipe to 38 mm. We repeated analysis of the dipole HOMs spectrum for modified geometry of the

3.9 GHz cavity End Group. The results are presented in Table 4 and Fig. 5 respectively. In consequence of this, the total number of nearby dipole HOMs is reduced to four only and the frequency of the closest dipole mode is shifted up by 100 MHz comparing to the original XFEL design.

THE HOM COUPLER NOTCH FILTER

An experimental scheme of measuring S-parameters of the 3.9 GHz cavity is illustrated in Fig. 6. Tuning of the HOM coupler notch filter is a non-trivial procedure, since direct measurements of transmitted signal through HOM ports are overlapped with cavity resonances. Thus, the notch filter maximum rejection is not visible on direct S_{13} and S_{24} curves. The solution is a normalization of HOM port signals to the signal transmitted from the main coupler to the field pick-up probe, which includes all cavity resonances but has no a notch filter on its way

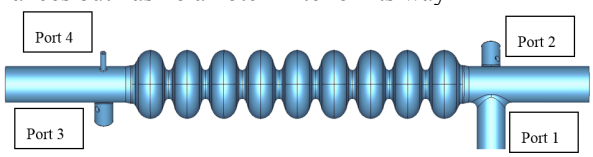

Figure 6: Scheme of the S-parameters measurement.

For an accurate reproducing of the experimental data in simulations, we use the scattering matrices decomposition technique [7]. Parameters of the decomposition scheme are presented in Fig. 7. The cavity is split on non-resonant subcomponents: upstream and downstream End Groups and cavity medium half-cells. Individual S-matrix of each subcomponent is calculated with ANSYS HFSS and results are transferred to ANSYS Designer for a final concatenation of S-matrices.

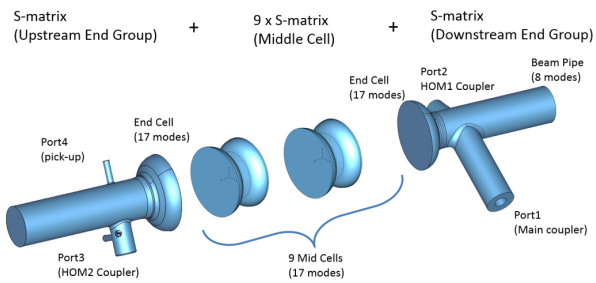

Figure 7: Scheme of the cavity S-matrix decomposition.

Based on a previous experience with HOM couplers tuning, tolerances of few MHz was observed for the notch filter central frequency in the XFEL 3.9 GHz cryomodule. Therefore, one can expect up to 1 W average RF power leak from the operating mode through the single HOM at nominal accelerating gradient of 14.9 MV/m (see Fig. 8). A simulated mechanical sensitivity of the notch filter central frequency to a deformation of the HOM coupler end cap is 2.4 MHz/μm. Next, the S-matrix of middle half-cells was found assuming there are 17 circular waveguide modes (up to the TM_{02} mode) in the cross section. Finally, we simulated signals transmission in the full 9-cell 3.9 GHz structure. The result of ANSYS Designer analysis is shown in Fig. 9 for signals transmitted from main coupler and downstream HOM coupler to the field pick-up port. Because the signal from the HOM coupler is heavily suppressed near the operating π-mode, it is difficult to find the exact location of the notch filter central frequency.

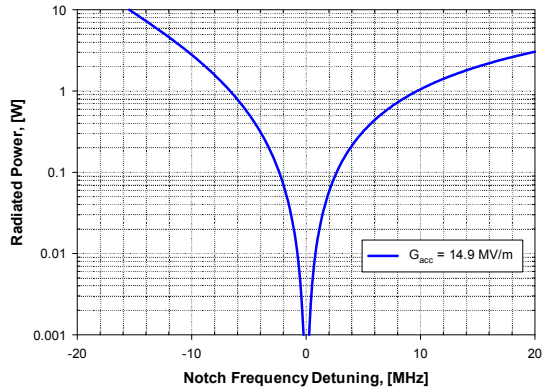

Figure 8: RF power radiated through the HOM-coupler.

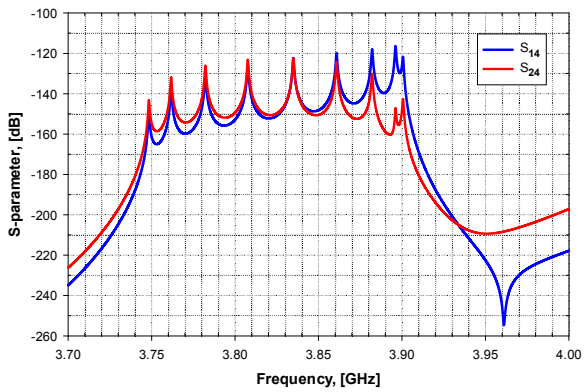

Figure 9: Signals transmission in the 3.9 GHz cavity.

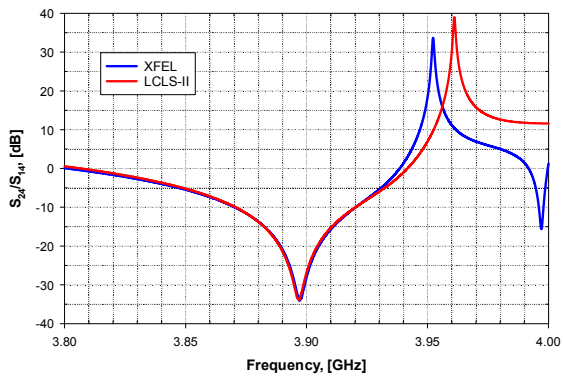

Figure 10: Notch filter passbands.

The reconstructed notch filter passbands are presented in Fig. 10 for the XFEL and LCLS-II 3.9 GHz cavities respectively. Evidently, the LCLS-II design with a reduced beam pipe aperture has a less influence of nearby dipole modes and, thus, provides an easy tuning of the sensitive HOM coupler notch filter.

CONCLUSIONS

The redesign of the 3.9 GHz cavity End Group is completed. Reduced beam pipe aperture simplifies the HOM coupler notch filter tuning, while modifications of the HOM coupler f-part and the antenna reduce RF losses in the HOM feedthrough making it suitable for CW operation of the LCLS-II linac.

ISBN 978-3-95450-169-4

REFERENCES

[1] *LCLS-II Final Design Report*, LCLSII-1.1-DR-0251, SLAC, 2015.

[2] *SCRF 3.9 GHz Cryomodule Physics Requirements Document*, LCLSII-4.1-PR-0097-R2, SLAC, 2016.

[3] T. Khabiboulline *et al.*, "3.9 GHz Superconducting Accelerating 9-cell Cavity Vertical Test Results", in Proc. of *22th Particle Accelerator Conference, PAC07*, Albuquerque, New Mexico, USA, 2007, paper WEPMN111.

[4] M. Awida, *et al.*, "On the Design of Higher Order Mode Antennas for LCLS II', in *Proc. 27th Linear Accelerator Conference, LINAC'14,* Geneva, Switzerland, 2014, paper OPP046.

[5] T. Khabiboulline, private communications, Apr. 2016.

[6] ANSYS HFSS, `http://www.ansys.com/`

[7] K. Gupta, R. Garg, R. Chadha, " *Computer aided design of microwave circuits*", Artech House, Dedham, 1981.